RSC Advances

Journal Name

ARTICLE

Structural, optical and magnetic tunability in $KBiFe_2O_5$ multiferroics

Received 00th January 20xx,
Accepted 00th January 20xx

DOI: 10.1039/x0xx00000x

www.rsc.org/

X. Z. Zhai,[a] H. M. Deng,[b] W. L. Zhou,[a] P. X. Yang,[a, *] J. H. Chu,[a] and Z. Zheng[c]

$KBiFe_2O_5$, a highly promising multiferroics for perovskite solar cells, has been fabricated using a one-step thermal treatment method. The resulting products were characterized by X-ray diffraction, scanning electron microscopy and ultraviolet–visible–near-infrared spectroscopy. The effect of temperature on the formation of $KBiFe_2O_5$ polycrystalline was assessed, and we found that the reaction temperature is the key factor in determining the optical property of the final products. Pure multiferroics $KBiFe_2O_5$ forms at a temperature of 850 °C with a narrow band gap 1.65eV, which is due to the stronger covalent in character of Fe-O in FeO_4 than that in FeO_6 accompanying the inverted t_{2g}/e_g orbitals of tetrahedral. The magnetic transition from paramagnetism to ferromagnetism corresponds to the site of Fe^{3+}, and the magnetic moment modification in ferromagnitic phase in $KBiFe_2O_5$ could be correlated with the temperature and distortion of unit cell. These results are helpful in the deeper understanding of relation between crystal structure and physical property in perovskite-like oxides and show the potential role, such materials can play, in perovskite solar cells and multiferroic applications.

Introduction

Ferroelectric materials, which are characterized by a spontaneous polarization that helps separate photon-generated charge carriers thus enhances photovoltaic effects and can be switched using an external electric field, have drawn enormous attention as a candidate class of materials for use in photovoltaic and other multifunctional devices [1-3]. Considering its potential applications in fundamental scientific research and in devices based on the mutual controls of magnetic and electric fields, the design and preparation of multiferroic materials have begun to generate great interest. However, multiferroics are still rare because the mechanisms driving for ferroelectricity and ferromagnetism are mutually exclusive based on theoretical consideration [4]. Recently, the discovery of large photovoltages up to 15V in multiferroics $BiFeO_3$ films has attracted increased attention to ferroelectrics photovoltaics [5]. However, most of the current ferroelectrics oxides have wide band-gap (Eg> 2.7 eV for $BiFeO_3$, Eg> 3.5 eV for PZT) that are beyond the visible-light range and thus allow the use of only 8% ~ 20% of solar spectrum [6, 7], which may be one of the major obstacles that limit the photovoltaic application of ferroelectrics. Therefore, identifying approaches to reducing the band gap of ferroelectrics without losing the useful ferroelectricity will bring significant scientific and technological breakthroughs with complex metal oxides.

To search for such materials, over the past few years, the band gap-engineering concept has been proposed, including doping the TiO_6 network with an oxygen-vacancy-stabilized d^8 M^{2+}(M = Ni, Pd, Pt, and Ce), and the realization of lower Eg to below 2.0 eV [8, 9]. Some studies suggested increasing tetragonality in $Bi(Zn_{1/2}Ti_{1/2})O_3$ and inserting layered B cations may suppress oxygen octahedral rotation thus reducing Eg to 1.48 eV [10], but only in theory. Moreover, reduced oxygen coordination (d^n MO_{6-x}, x being 1 or 2) could offer another strategy to achieve low E_g ferroelectrics [11], attributed to the lack of inversion symmetry of tetrahedral compounds compared with octahedral compounds. Smaller coordination number and the inverted t_{2g}/e_g orbitals of tetrahedral compounds also lead to a smaller Eg. Perovskite oxide ABO_3 is composed of a three-dimensional framework of corner-sharing BO_6 octahedra, which controls the most of the properties of perovskite oxides [12-14]. However, anion vacancy ordering may lead to the formation of superstructures that are intergrowths of perovskite and oxygen-deficient perovskite layers. A sequence of idealized structures canthus be viewed as composed of $A_nB_nO_{3n-1}$ phases with end members $A_2B_2O_5$ (n = 2) and ABO_3 (n=∞), where (n – 1) layers of BO_6 octahedra alternate with one layer of BO_4 tetrahedra [15]. The brownmillerite structure $A_2B_2O_5$ is a kind of oxygen-deficient perovskite structure, which is composed of perovskite-like three-dimensional framework of corner-sharing BO_6 octahedra alternating with slabs containin grows of corner-sharing BO_4 tetrahedra, formed by the deficiency of oxygen during the formation of the structure [16-18], namely, a structural model for $A_2B_2O_5$ can be derived

a. Key Laboratory of Polar Materials and Devices, Ministry of Education, Department of Electronic Engineering, East China Normal University, Shanghai 200241, China
b. Instrumental Analysis and Research Center, Institute of Materials, Shanghai University, 99 Shangda Road, hanghai 200444, China
c. Key Laboratory for Micro-Nano Energy Storage and Conversion Materials of Henan Province, Institute of Surface Micro and Nano Materials, Xuchang University, Henan 461000, China

from the perovskite structure ABO_3 by removing 1/6 of the oxygenin ordered rows [19]. Brownmillerite has been studied extensively as a kind of promising photocatalyst due to their narrower band gap [20] (often less than 3.0 eV) which can be easily excited under visible light or UV light irradiation. Recently, Zhang *et al*. [11] reported a new multiferroic $KBiFe_2O_5$ crystal structure which contains tetrahedral Fe^{3+} in a $[Fe_2O_3]$ block that alternates with a $[(K, Bi)O_2]$ block, using a typical solvent-thermal synthesis procedure. Exploratory characterization of this compound found a much lower Eg, 1.6 eV and promising dielectric, ferroic and photosensitive properties. In spite of intensive investigations, the new synthesis methods and physical property are still worth further exploring.

In this paper, we developed a non-toxic, low-cost and simple way to fabricate the multiferroics $KBiFe_2O_5$ as absorber layers for photovoltaic application, using a one-step thermal treatment method. The crystal structure, surface morphology, optical and magnetic properties of $KBiFe_2O_5$ have been studied as a function of temperature up to 950 °C. As the literature indicated [21], the physical and chemical properties of the materials are considerably affected by the characteristics of purity, size and morphology. These results then are used to gain insight into the origin and understanding of relation between crystal structure and physical property in perovskite-like brownmillerite ($A_2B_2O_5$) materials, which provide great potential applications in optoelectronic and solar energy devices.

Experimental

Multiferroics $KBiFe_2O_5$ was prepared by a solid-state reaction method [22-23]. The main process is as follows: K_2CO_3 (99.5%), Bi_2O_3 (99.5%) and Fe_2O_3 (99.5%) were used as starting raw materials. The starting materials were weighed in required molar rations and ball-milled in an alcohol medium with zirconia balls (5% of excess Bi and K were added to compensate for loss during the heat treatment). The dried slurries were sintered at the temperature range 650–950 °C for 4 h using box-type annealing furnace for the synthesis of $KBiFe_2O_5$ sample. The thermogravimetric analysis (TGA) was performed on a thermal gravimetric analyzer in N_2 flow and the heating rate of 5 $°C\cdot min^{-1}$. The crystalline structure of the $KBiFe_2O_5$ polycrystallines were investigated by X-ray diffraction (XRD, Bruker D8 Advance) with Cu-Kα radiation source. In the XRD measurement a continuous scanning mode (θ ~ 2θ) were selected with a step size of 0.2° and collection time of 0.1s. The surface morphology of the $KBiFe_2O_5$ polycrystallines was examined by scanning electron microscopy (SEM, Philips XL30FEG). The optical transmittance experiments were carried out by the ultraviolet-visible-near-infrared (UV-vis-NIR) spectrophotometer (cary500, USA Varian). The magnetic properties of the samples were invested by physical property measurement system (PPMS-9, Quantum Design). All the measurements were at room temperature.

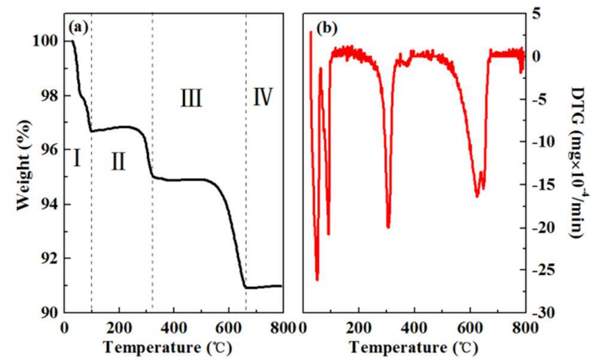

Figure 1 (a) TGA and (b) DTG graphs of multiferroics $KBiFe_2O_5$ polycrystalline.

Results and discussion

Although previous Zhang *et al*. [11] has synthesized multiferroics $KBiFe_2O_5$ single crystal using a typical solvent-thermal synthesis procedure, the grown process of $KBiFe_2O_5$ has not been focused on. In present study, $KBiFe_2O_5$ crystals were synthesized by a simple and low-cost solid-state reaction method. To understand how the reaction paths affect the formation of $KBiFe_2O_5$ crystals, we investigated the influence of the synthesis temperature on the formation of $KBiFe_2O_5$ crystals. As shown in Figure (1), the thermogravimetry and differential thermogravimetry (TG-DTG) were done in the range of 25-800°C for confirming the proper synthesis temperature, and three obvious weight loss processes were elucidated, and total weight loss was observed - 91%. The first mass loss before 100°C (~ 3.2%) is resulted from evaporation of moisture contents. The second weight loss (~ 1.8%) between100 °C and 320 °C is mainly ascribed to the presence of water molecules inside the pores of the polycrystalline. The third obvious weight loss (~ 4.1%) is located at 320°C ~ 650°C because of the volatilization of CO_2 and conversion of binary and ternary metal oxides to target compound. When the temperatures higher than 650 °C, no discernible weight loss is observed, indicating that the metal oxides is starting to transform into $KBiFe_2O_5$. So we conclude that the lowest synthesis temperature for $KBiFe_2O_5$ is 650 °C.

Room-temperature XRD patterns of the as-prepared samples at different synthesis temperatures are shown in Figure (2). These XRD data show the samples to be consistent with a polycrystalline like-perovskite structure, which is similar to Zhang's results [11], at least within the detection limits of the instrument. In Figure (2), a slight impurity peaks marked by special symbol have been observed in $KBiFe_2O_5$, which corresponds to KBiO*x*. The absence of impurity phases for samples at 650 and 750°C indicates that 750°C is not high enough for the $KBiFe_2O_5$ to be well crystallized, namely, binary oxide and ternary oxide could not transform into $KBiFe_2O_5$ completely below the 850°C. Moreover, it is notable that the

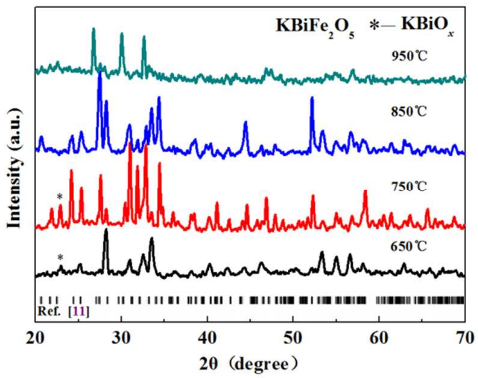

Figure 2 XRD patterns of $KBiFe_2O_5$ polycrystallines with different synthesis temperatures.

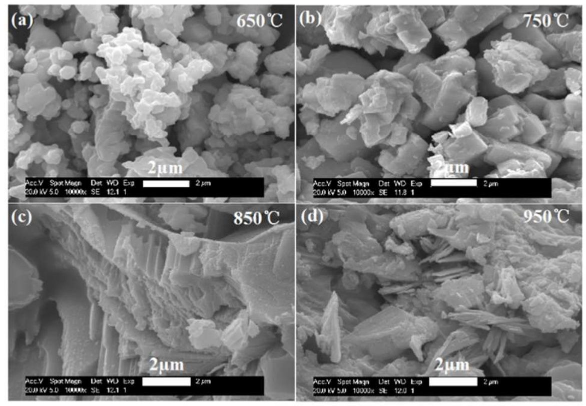

Figure 3 SEM micrographs of $KBiFe_2O_5$ polycrystallines with different synthesis

number and intensity of the peaks decreased sharply when the temperature increased at 950°C. Since almost no JCPDS files (Joint Committee for Powder Diffraction Standards) for new multiferroic $KBiFe_2O_5$ are available, within the scope of our cognitive, the structure of $KBiFe_2O_5$ film was investigated in our work based on Ref. 11. We could not explained this peaks decreased phenomenon exactly, and we just speculated the reasons for this phenomenon within the scope of my ability is as follows: the decomposition of the $KBiFe_2O_5$ at the higher temperature, the occurrence of phase transition and the different preferred orientation growth of polycrystalline material $KBiFe_2O_5$. From the XRD results, we concluded that 850°C is the optimal temperature for forming the pure $KBiFe_2O_5$ polycrystalline in our experiment. The EDX analysis results of the $KBiFe_2O_5$ show that 850°C is most close to the standard molar ratio 1 : 1 : 2 for Bi : K : Fe (in at.%), which agrees with the above XRD analysis.

Figure (3) show the typical SEM images of the as-prepared $KBiFe_2O_5$ polycrystalline material obtained at 650°C, 750°C, 850°C and 950°C, respectively. The morphological differences have been clearly observed in $KBiFe_2O_5$ polycrystalline at different synthesis temperatures. Numerous grains, about 400~500nm in diameter, agglomerated irregularly are observed in $KBiFe_2O_5$ at 650°C, as seen the Figure3 (a). However, the grains size larger into micrometer scale blocks structure at 750°C. As the temperature increased up to 850°C, the micrometer scale block structure agglomerated layer by layer. The obvious laminar microstructure was observed in Figure3(c). The laminar microstructure structure collapses when the synthesis temperature is up to 950°C, as seen in Figure3 (d). It can be clearly observed that the particles microstructure present a transition from grains to laminar.

Figure 4(a) shows the optical absorption spectra of the $KBiFe_2O_5$ polycrystalline with different synthesis temperatures using UV-vis-NIR spectrophotometer. As shown in Figure 4(a), the UV-Vis absorption spectra presented very noisy spectra, which may be caused by the impurity phase in the $KBiFe_2O_5$ sample. The curves with the lowest noisy are corresponding to the sample at the optimal synthesis temperature 850°C, which is consistent with XRD results. The optical transmittance properties are relevant to the electronic structure features and band gap. It is apparent that the band gap absorption edges of the samples exhibit a drastic red-shift with increasing the synthesis temperatures until at 850°C, the sample at 850°C has better light absorption in the visible wavelength range. The corresponding optical band gaps (E_g) of $KBiFe_2O_5$ can be estimated from the tangent lines in the plot of the Kubelka-Munk function $(\alpha h\nu)^2$ versus $h\nu$ for the direct band gap material, where α is a absorbance and $h\nu$ is photon energy [24]. As presented in the Figure 4(b), the slope of the linear part suggests the band gap of which agrees with that $KBiFe_2O_5$ polycrystalline at 850°C is estimated to be 1.65eV,reported in prior studies [11], and that of the other three $KBiFe_2O_5$ polycrystalline are 2.07 eV, 1.75 eV and 1.97eV for 650°C, 750°C and 950°C, respectively. It can be seen that the band gap presents a non-linear change with the temperature, with an initial steep decline for temperature from 650°C to 850°C, then a remarkable raise at 950°C, as seen in Figure 4 (c). In the fundamental absorption edges regions, the absorption is due to the band-to-band transition from the top of valence band (VB) to the bottom of the conduction band (CB) directly. For $KBiFe_2O_5$, the top of VB arises mainly from the O 2*p* orbitals and the bottom of the CB is essentially set by the Fe^{3+} 3*d* ($e_g t_{2g}$) orbitals. $KBiFe_2O_5$ polycrystalline presents a sharply lower band gap, which can be due to a distorted crystal field at the tetrahedral environment leading to the further splitting of the t_{2g} and e_g and their orbital inversions [11].

Compared with the ferroelectric ABO_3 perovskites with BO_6 octahedral, for instance, $BiFeO_3$ (~2.7eV) [25], the $KBiFe_2O_5$ (1.65eV) has an ideal band-gap for the perovskite solar cells. This narrowing band-gap behavior in our work can be explained by the mechanism of FeO_4 tetrahedral effect. Local chemistry bonding and crystal field theory were investigated to understand this FeO_4 tetrahedral effect, within the scope of our ability. For $KBiFe_2O_5$, each Fe forms a distorted oxygen tetrahedron with four Fe-O bonds in the range of 1.801–1.916Å [11], which are shorter than six Fe–O bonds, forms a distorted oxygen octahedral in $BiFeO_3$ [26]. And the distorted $[BiO_6]^{9-}$ octahedra with four Bi–O bond lengths are within

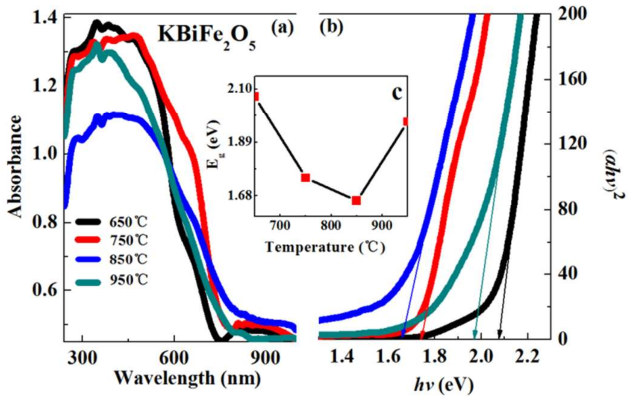

Figure 4 (a) The UV-vis-NIR absorption spectra of the as-synthesis $KBiFe_2O_5$ polycrystalline with different synthesis temperatures (b) plots of $(\alpha h\nu)^2$ versus hν for the absorption spectra. (c) Eg values versus temperatures for $KBiFe_2O_5$ polycrystalline.

2.130–2.345 Å and the other two at 2.712 Å and 2.809 Å. Similarly dispersive metal-oxygen distances are common for Bi^{3+}-containing compounds due to lone pair electrons [27]. As we know, bonding between the oxygen and iron atoms at the tetrahedral site was more covalent in character than at octahedral site [28]. The strong covalent character of the tetrahedral sites would be one of the reasons for narrower band-gap in $KBiFe_2O_5$. From a qualitative stand point, the crystal field splitting energy in a tetrahedral field is normally smaller than that in an octahedral field for the same ion species [28]. And the electron pairing energy is higher than crystal field splitting energy for tetrahedral field, which resulted in the electrons are hardly in pair in tetrahedral field. For the $KBiFe_2O_5$ polycrystalline, the distorted crystal field at the tetrahedral environment leads to the further splitting of the t_{2g} and e_g orbits, which were inversion compared with that at the octahedral environment. Since the Fe^{3+} ions nominally has five d-electrons, half of the 3d-band of Fe is occupied with electrons having the same spin, which resulted in an increase density of states in the conduntion band accompanied by the occurrence of localized states in band gap. The differences between the local electronic structure of FeO_6 octahedra and FeO_4 tetrahedra would be one of the reasons for narrowing band-gap in the FeO_4 tetrahedra for $KBiFe_2O_5$.

Finally, the magnetization versus magnetic field (*M-H*) curves of $KBiFe_2O_5$ polycrystalline measured with a maximum magnetic field of 10 kOe at room temperature is shown in Figure 5(a)-(d). For the sample at 650°C, in which Fe atoms do not occupy FeO_4 tetrahedral site, the linear *M-H* curve is obtained, demonstrating that the samples is paramagnetic. But because of synthesis temperatures increasing, the paramagnetic contributions disappear and a S-type hysteresis for ferromagnetic materials is obtained, indicating the emergence of weak ferromagnetic long-range ordering in

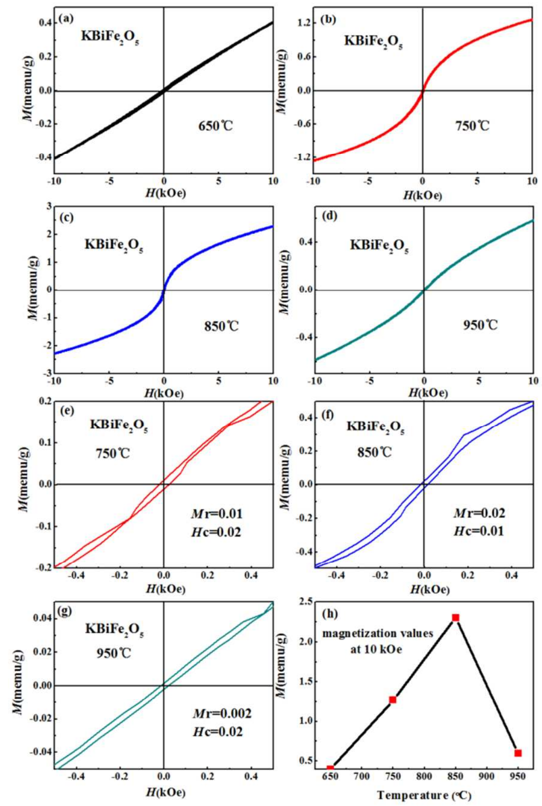

Figure 5 *M-H* data hysteresis of $KBiFe_2O_5$ polycrystalline with different synthesis temperatures: (a) 650°C, (b) 750°C, (c) 850°C, (d) 950°C. The zoom-in images of *M-H* hysteresis of $KBiFe_2O_5$ polycrystalline with different synthesis temperatures: (e) 750°C, (f) 850°C, (g) 950°C. (h) Magnetization values at 10 kOe versus synthesis temperatures for $KBiFe_2O_5$ polycrystalline.

$KBiFe_2O_5$ polycrystalline material, as seen in Figure 5(b)-(d). The zoom-in images of *M-H* hysteresis of $KBiFe_2O_5$ polycrystalline with different synthesis temperatures were shown in Figure 5(e)-(g). The remanent magnetization (*M*r) are 0.01, 0.02, and 0.002 emu/g, and the coercive field *H*c are 0.02, 0.01, and 0.02 kOe for the samples Figure 5(e)-(g)). The magnetization values at 10 kOe were shown in Figure 5(h). The magnetization values show a linear increase with the synthesis temperatures from 650°C to 850°C and have a sharp decrease with the synthesis temperatures from 850°C to 950°C, as seen in Figure 5(h). The maximum magnetization value at 10 kOe, 2.3 emu/g, has been also observed for the sample obtained at 850°C.

Since K^{+} and Bi^{3+} are both nonmagnetic, these magnetic features must be attributed to the Fe atoms. The origin of magnetism is due to the exchange interaction between local-spin polarized electrons and conduction electrons. This interaction leads to the spin polarization of conduction electrons. Subsequently, the spin polarization conductive electrons perform an exchanges interaction with spin-polarized electrons of other Fe ions. Thus, after the long-range exchange interaction, almost all Fe moment align in the same direction, inducing ferromagnetic in material [29-33]. The magnetism of the system depends on the competition among the thermal motion, the order energy and the cold-disorder energy. For the samples at 650°C, in which Fe atoms do not occupy FeO_4 tetrahedral site, attributing to the binary oxide and ternary oxide have not transformed into $KBiFe_2O_5$. Since the larger thermal motion energy, almost all Fe moment with different directions were offset and the net magnetic moment is zero, the consistency of internal spin was induced by the applied magnetic field. So, the sample at 650°C shows paramagnetic. With further increase of the synthesis temperatures, lattice defect such as oxygen vacancies is easily formed in $KBiFe_2O_5$ polycrystalline, acting as shallow donors. So the $KBiFe_2O_5$ polycrystalline obtained at 750°C, 850°C and 950°C show weak ferromagnetism.

The Fe^{3+} ions now occupy FeO_4 tetrahedral site, the comparable crystal field splitting energy and spin-spin exchange splitting energy leads to spin state transition, namely, controls the valence electron which can adjust the modification of the magnetic moments. In the tetrahedral crystal field, Fe^{3+} may have three different spin state configuration; high spin (HS, S =5/2, $t_{2g}^3e_g^2$), intermediate spin (IS, S = 3/2, $t_{2g}^4e_g^1$) and low spin (LS, S = 1/2, $t_{2g}^5e_g^0$). The samples annealed at 750 °C shows a better hysteresis loop due to Fe^{3+} IS state in $KBiFe_2O_5$ (as seen in Figure 5b), and the samples annealed at 850 °C shows a best hysteresis loop due to Fe^{3+} HS state in $KBiFe_2O_5$(as seen in Figure 5c), but the samples annealed at 950 °C shows a decreased magnetic moment due to Fe^{3+} LS state in $KBiFe_2O_5$(as seen in Figure 5d), which further confirms that 850 °C is the most suitable temperature to synthesize high-performance $KBiFe_2O_5$. In addition, it can also be observed that the magnetism transition from paramagnetism to ferromagnitism corresponds to the site of Fe^{3+}, the magnetic moment modification in ferromagnetic phase in $KBiFe_2O_5$ could be correlated with the temperature and distortion of unit cell.

Conclusions

In summary, $KBiFe_2O_5$ polycrystalline have been successfully fabricated using a one-step thermal treatment method. The temperature effect on the morphology and crystal structure of $KBiFe_2O_5$were investigated, and the reaction temperature was found to pay a critical role in the formation of the final production. $KBiFe_2O_5$ polycrystalline form at a temperature of 850 °C with a narrow band gap 1.65eV, which is due to the stronger covalent in character of Fe-O in than that in FeO_6 accompanying the inverted t_{2g}/e_g orbital of tetrahedral. The magnetism transition from paramagnetic to ferromagnetic corresponds to the site of Fe^{3+}, and the magnetic moment modification in ferromagnetic phase in $KBiFe_2O_5$ could be correlated with the temperature and distortion of unit cell. These results are helpful in the deeper understanding of relation between crystal structure and physical property in perovskite-like oxides and show the potential role, such materials can play, in perovskite solar cells and multiferroic applications.

Acknowledgements

This work was supported by the National Natural Science Foundation of China (61474045), the State Key Basic Research Program of China (2013CB922300).

Notes and references

1 H. T. Huang, Nat. Photonics Solar energy: Ferroelectric photovoltaics, 2010, **4**, 134-135.
2 T. Choi, S. Lee, Y. J. Choi, V. Kiryukhin and S. W. Cheong, Science Switchable ferroelectric diode and photovoltaic effect in $BiFeO_3$, 2009, **324**, 63-66.
3 T. Lottermoser, T. Lonkai, U. Amann, D. Hohlwein, J. Ihringer and M. Fiebig, Nature (London) Magnetic phase control by an electric field, 2004, **430**, 541-544.
4 W. Eerenstein, N. D. Mathur and J. F. Scott, Nature Multiferroic and Magnetoelectric Materials, 2006, **442**, 759-765.
5 S. Y. Yang, J. Seidel, S. J. Byrnes, P. Shafer, C. H. Yang, M. D. Rossell, P. Yu, Y. H. Chu, J. F. Scott, J. W. Ager, L. W. Martin and R. Ramesh, Nature Nanotech. Above-bandgap voltages from ferroelectric photovoltaic devices, 2010, **5**, 143-147.
6 I. Grinberg, D. V. West, M. Torres, G. Gou, D. M. Stein, L. Wu, G. Chen, E. M. Gallo, A. R. Akbashev, P. K. Davies, J. E. Spanier and A. M. Rappe, Nature Perovskite oxides for visible-light-absorbing ferroelectric and photovoltaic materials, 2013, **503**, 509.
7 W. S. Choi, M. F. Chisholm, D. J. Singh, T. Choi and G. E. Jellison Nat. Commun. Wide bandgap tunability in complex transition metal oxides by site-specific substitution, 2012, **3**, 689.
8 J. W. Bennett, I. Grinberg and A. M. Papper, J. Am. Chem. Soc. New highly polar semiconductor ferroelectrics through d^8 cation-O vacancy substitution into $PbTiO_3$: Atheoretical study, 2008, **130**, 17409-17412.
9 J. W. Bennett, I. Grinberg, P. K. Davies and A. M. Papper, Phys. Rev. B. Pb-free semiconductor ferroelectrics: A theoretical study of Pd-substituted Ba $(Ti_{1-x}\ Ce_x)\ O_3$ solid solutions, 2010, **82**, 184106.
10 T. Qi, I, Grinberg and A. M. Papper Phys. Rev. B. Band-gap engineering via local environment in complex oxides, 2011, **83**, 224108.
11 G. H. Zhang, H. Wu, G. B. Li, Q. Z. Huang, C. Y. Yang, F. Q. Huang, F. H. Liao and J. H. Lin, Scientific Reports New high Tc multiferroics $KBiFe_2O_5$ with narrow band gap and promising photovoltaic effect, 2013, **3**, 1265.
12 J. Wang, J. B. Neaton, H, Zheng, V, Nagarajan, S. B. Ogale, B. Liu, D. Viehland, V. Vaithyanathan, D. G. Schlom, U. V. Waghmare, N. A. Spaldin, K. M. Rabe, M. Wutting and R. Ramesh Science Epitaxial $BiFeO_3$ multiferroic thin film heterostructures, 2003, **299**, 1719-1722.
13 A. Moreira dos Santos, S. Parashar, A. R. Raju, Y. S. Zhao, A. K. Cheetham and C. N. R. Rao, Solid State Commun. Evidence for the likely occurrence of magnetoferroelectricity in the simple perovskite $BiMnO_3$, 2002, **122**, 49-52.
14 T. Kimura, T. Goto, K. Thizaka, T. Arima, and Y. Tokura, Nature Magnetic control of ferroelectric polarization, 2003, **426**, 55-58.
15 P. Berastegui, S. G. Eriksson and S. Hull Mater. Res. Bull. A Neutron diffraction study of the temperature dependence of $Ca_2Fe_2O_5$, 1999, **34**, 303–314.
16 S. Shin, M. Yonemura, H. Ikawa, Mater. Res. Bull. Order disorder transition of $Sr_2Fe_2O_5$ from brownmillerite to perovskite structure at elevated temperature, 1978, **13**, 1017-1021.

17 J. B. Goodenough, J. E. Ruiz-Diaz, Y. S. Zhen, Solid State Ionics Oxide-ion conduction in $Ba_2In_2O_5$ and $Ba_3In_2MO_8$ (M=Ce, Hf, or Zr), 1990, **44**, 21-31.
18 S. Tanasescu, N. D. Totir and D. I. Marchidan Solid State Ionics Thermodynamic Properties of the $SrFeO_{2.5}$ and $SrMnO_{2.5}$ Brownmillerite-Like Compounds by Means of EMF-Measurements, 2000, **134**, 265-270.
19 P. Berastegui, S. G. Eriksson and S. Hull, Mater. Res. Bull. A Neutron Diffraction Study of the Temperature Dependence of $Ca_2Fe_2O_5$, 1999, **34**, 303-314.
20 Y. Yang, Z. Q. Cao, Y. S. Jiang, L. H. Liu and Y. B. Sun Mater. Sci. Eng. B Photoinduced structural transformation of $SrFeO_3$ and $Ca_2Fe_2O_5$ during photodegradation of methyl orange, 2006, **132**, 311-314.
21 X. M. Xu, S. D. Li, X. L. Wang, Y. T. Ma, X. H. Wang and K. Gao, Mater. Lett. Fabrication and characterization of $Ca_2Fe_2O_5$ nanofibers photocatalyst by sol-gel assisted electrospinning at low-temperature, 2015, **143**, 75-79.
22 B. H. Jun, J. H. Kim, C. J. Kim, K. N. Choo, J. Alloys. Compd. Improved transport critical current properties in glycerin-doped MgB_2 wire using milled boron powder and a solid-state reaction of 600 °C, 2015, **650**, 794–798.
23 B. Zhao, Y. Tong, Y. Zhao, T. Yang, F. Yang, Q. Hu, C. Zhao, Ceramics International Preparation of ultra-fine Sm0.2Ce0.8O1.9 powder by a novel solid state reaction and fabrication of dense Sm0.2Ce0.8O1.9 electrolyte film, 2015, 41, 9686–9691.
24 J. He, L. Sun, S. Y. Chen, Y. Chen, P. X. Yang and J. H. Chu, J. Alloys. Compd. Composition dependence of structure and optical properties of $Cu_2ZnSn(S,Se)_4$ solid solutions: An experimental study, 2012, **511**, 129-132.
25 D. J. Huang, H. M. Deng, P. X. Yang, J. H. Chu, Mater. Lett. Optical and electrical properties of multiferroic bismuth ferrite thin films fabricated by sol-gel technique, 2010, **64**, 2233-2235.
26 A. Palewicz, I. Sosnowska, O. R. Przenios and A. W. Hewat, Acta Phys. Pol. A $BiFeO_3$ crystal structure at low temperatures, 2010, **117**, 296-301.
27 J. Yang and M. J. Dolg, J. Phys. Chem. B First-Principles Electronic Structure Study of the Monoclinic Crystal Bismuth Triborate BiB_3O_6, 2006, **110**, 19254-19263.
28 M. Haruta, H. Kurata, K. Matsumoto, S. Inoue, Y. Shimakawa and S. Isoda, J. Appl. Phys. Local electronic structure analysis for brownmillerite $Ca(Sr)FeO_{2.5}$ using site-resolved energy-loss near-edge structures, 2011, **110**, 033708.
29 A. F. Jalbout, H. Chen and S. L. Whittenburg, Appl. Phys. Lett. Monte Carlo simulation on the indirect exchange interactions of Co-doped ZnO film, 2002, **81**, 2217.
30 F. Matsukura, H. Ohno, A. Shen, and Y. Sugawara, Phys. Rev. B. Transport properties and origin of ferromagnetism in (Ga,Mn)As, 1998, **57**, R2037.
31 J. MD. Coey, M. Venkatesan and C. B. Fitzgerald, Nat. Mater Donor impurity band exchange in dilute ferromagnetic oxides, 2005, **4**, 173-179.
32 W. L. Zhou, H. M. Deng, P. X. Yang and J. H. Chu, Appl. Phys. Lett. Structural phase transition, narrow band gap, and room-temperature ferromagnetism in $[KNbO_3]_{1-x}[BaNi_{1/2}Nb_{1/2}O_3]_x$ ferroelectrics, 2014, **105**, 111904.
33 W. L. Zhou, H. M. Deng, L. Yu, P. X. Yang and J. H. Chu, J. Appl. Phys. Magnetism switching and band-gap narrowing in Ni-doped $PbTiO_3$ thin films, 2015, **117**, 194102.

